A Novel yet Simple Approach to the Interpretation of HVSR Data in Australia – A Data Rich Case Study from the Pilbara

Nathan Tabain
BHP
Nathan.tabain@bhp.com

Remke van Dam
Southern Geoscience Consultants
remke.vandam@sgc.com.au

SUMMARY

Two passive seismic surveys were acquired at a location within the Hamersley Basin in the Pilbara region of Western Australia, to assist BHP with optimisation of both drill planning for managed aquifer recharge studies, and for iron ore exploration drilling. The geology of the target area consists of stratigraphic metasediments, which have been intruded, faulted, folded, eroded, and then mostly covered by thin to moderate thickness tertiary detrital cover.

Following review of various airborne geophysical datasets, two passive seismic surveys were planned across the target location with the primary objective of better defining the thickness of detrital cover. The passive seismic surveys consisted of three-component nodal geophones being deployed in a rolling manner at ~3,400 stations. The data were processed using the empirical horizontal-to-vertical spectral ratio (HVSR) method.

Interpretations from various apriori unpublished passive seismic surveys and trials across the Pilbara using this method have returned mixed results, with the consistency and continuity of HVSR horizons along and between survey lines being one of the primary concerns.

When reviewing the processed HVSR data, it was observed that a HVSR trough/ resonance minimum typically produced a vertically more discrete and laterally consistent horizon, with more depth variability than the traditionally picked HVSR peaks. The trough horizon also produced steeper dipping and paleochannel-like features, which are known to exist in the survey area and were largely absent from the HVSR peak/ maximum horizons.

The HVSR trough horizon was picked for all passive seismic stations, where present, and when gridded into a surface using half the picked frequency, it correlated well with various geological features previously interpreted from the airborne magnetic, gravity gradiometry and electromagnetic data. This surface is being used to inform managed aquifer recharge modelling and drill planning and optimise future exploration drill planning.

Key words: Geophysics, Passive Seismic, HVSR, Trough, Interpretation

INTRODUCTION

BHP Western Australia Iron Ore (WAIO) is studying its options for both groundwater abstraction and managed acquire recharge (MAR) of surplus water at a location within the Hamersley Basin, in the Pilbara region of Western Australia. The area is covered by apriori airborne geophysical datasets supported by limited drilling and geological mapping. The thickness of the cover is largely unknown, particularly within the large paleochannels. Following review of the various apriori airborne geophysical datasets, two passive seismic surveys were planned across the target location with the primary objective of better defining the thickness of detrital cover. The intent is to use this information to inform hydrogeological conceptualisation of the area, and to optimise the placement of hydrogeological drill holes.

Passive seismic surveys using the horizontal-to-vertical spectral ratio (HVSR) method are frequently used to estimate the depth of bedrock (e.g., Lane et al., 2008). Conventional interpretation of HVSR data involves the picking of HVSR resonance peaks, whose frequencies are then converted to depths using a simple equation. This method has historically produced mixed results in the Pilbara, where density and velocity contrasts are relatively small and the geology/ geometry complex.

There is significant faulting and folding of the 2.5 km thick Hamersley Group (ca 2.5 Ba) stratigraphic meta sediments located in the Hamersley Basin, with BHP WAIO recognising 5 different major events (Kepert, 2018). Major structures are frequently intruded by dolerite dykes. Faults and joints are typically associated with weathering resulting in magnetite oxidising to hematite (Duuring et. al., 2019), increased porosity due to leaching of silica and reduced conductivity due to oxidisation of pyrite within shales. The geology of the survey area is comprised of stratigraphic meta-sediment basement: the Marra Mamba (MM) and Brockman (BKM) Banded Iron Formations (BIF) and the

Wittenoom Dolomite (WD), which have been intruded, faulted, folded and eroded (Figure 1). Most of the stratigraphic units are under cover, with several relatively deep, predominantly east - west trending paleochannels.
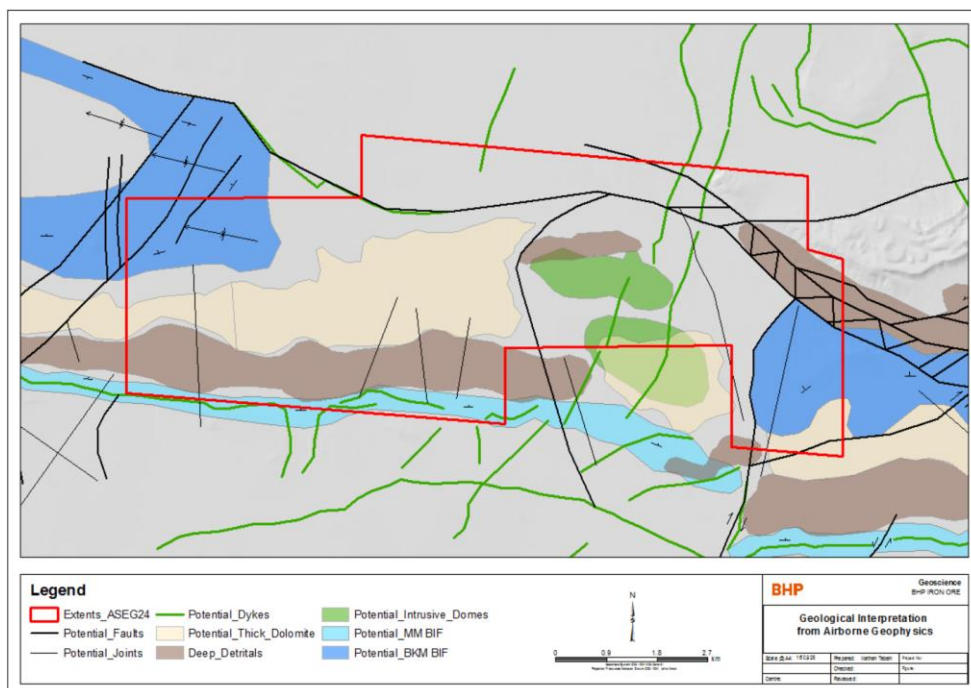

Figure 1. Integrated under-cover geological interpretation of apriori airborne geophysical datasets. Derived primarily from AMAG, AGG and AEM (Figure 2), supported by limited drilling and geological mapping. Passive seismic survey outline in red. Note that coordinates have deliberately been omitted.

APRIORI GEOPHYSICAL DATA & GEOLOGICAL INTERPRETATION

Airborne Gravity Gradiometry (AGG) data (Figure 2) were collected using a mixture of the HELIFALCON and FALCON systems, with 100 and 200 m line spacing respectively. AGG maps contrasts in near-surface density gradients, with WD and BIF typically presenting as density highs, whilst thick cover/ paleochannels present as lows, resulting in the ability to map both stratigraphy and indicate relative cover thickness.

Airborne magnetic (AMAG) data (Figure 2) were collected using a mixture of rotary-wing and fixed-wing platforms with 100 and 200 m line spacing, respectively. BIF, intrusions and some detritals show as highly magnetic (inclusion of magnetite and maghemite, respectively), whilst dolomite, chert and shale present as magnetic lows. Note that remanent magnetic field orientation must be considered, as highly magnetic geology frequently presents as strong magnetic lows in the Pilbara, when the remanent magnetic vector subtracts from Earth's present-day magnetic vector.

Airborne Electromagnetic (AEM) data (Figure 2) were collected using the TEMPEST system at 200 m line spacing. Once inverted for depth, this data can map electrical conductivity down to several hundred metres dependent upon the overlying lithology. Clay-rich cover and shale-rich stratigraphy typically present as highly conductive, whilst BIF and WD typically present as resistive, and the fresh-oxidised interface typically present. Note that the BKM and MM BIF are sandwiched between shale-rich, conductive stratigraphy. The base of oxidisation can often also be seen, with shales typically being more conductive when fresh. Note that groundwater within the Hamersley Basin is typically non-saline (BHP, 2023), and therefore is rarely visible in AEM data. Unfortunately, there is thick conductive clay-rich cover atop the largest paleochannel located in the southwest of the survey area, masking the conductive response from the shale-rich stratigraphy in the basement below.

The location has limited shallow exploration drilling in the BIF, and a handful of hydrogeological holes located in the paleochannel and WD located between the two main BIF units. Depth of cover varies from approximately 0 to 100 m, whilst in the paleochannel depths typically vary from 100 to 200 m. At one drillhole located in the east of the main paleochannel, basement was intercepted at approximately 400 m depth. One of the interpreted granitic intrusions was also intercepted by drilling. Due to limited basement outcrop, there is minimal geological mapping data available.

Prior to the passive seismic surveys, the above datasets were jointly interpreted to create a map of undercover major paleochannels, stratigraphy, structures, and intrusions throughout the area (Figure 1). In the southwest and east, there are large paleochannels, predominately incised between the MM in the south and WD where a shale-rich stratigraphic

unit has been preferentially eroded. The MM dips to the north, whilst both instances of BKM are structurally complex, with an asymmetrical syncline plunging to the east in the northwest, and gently dipping northward in the east. Many large dykes are evident to the south and northeast, along with two granitic domes in the centre. In the east and to the far north is a major fault zone, with cover to the north being very thick. Many other faults and joints are evident.
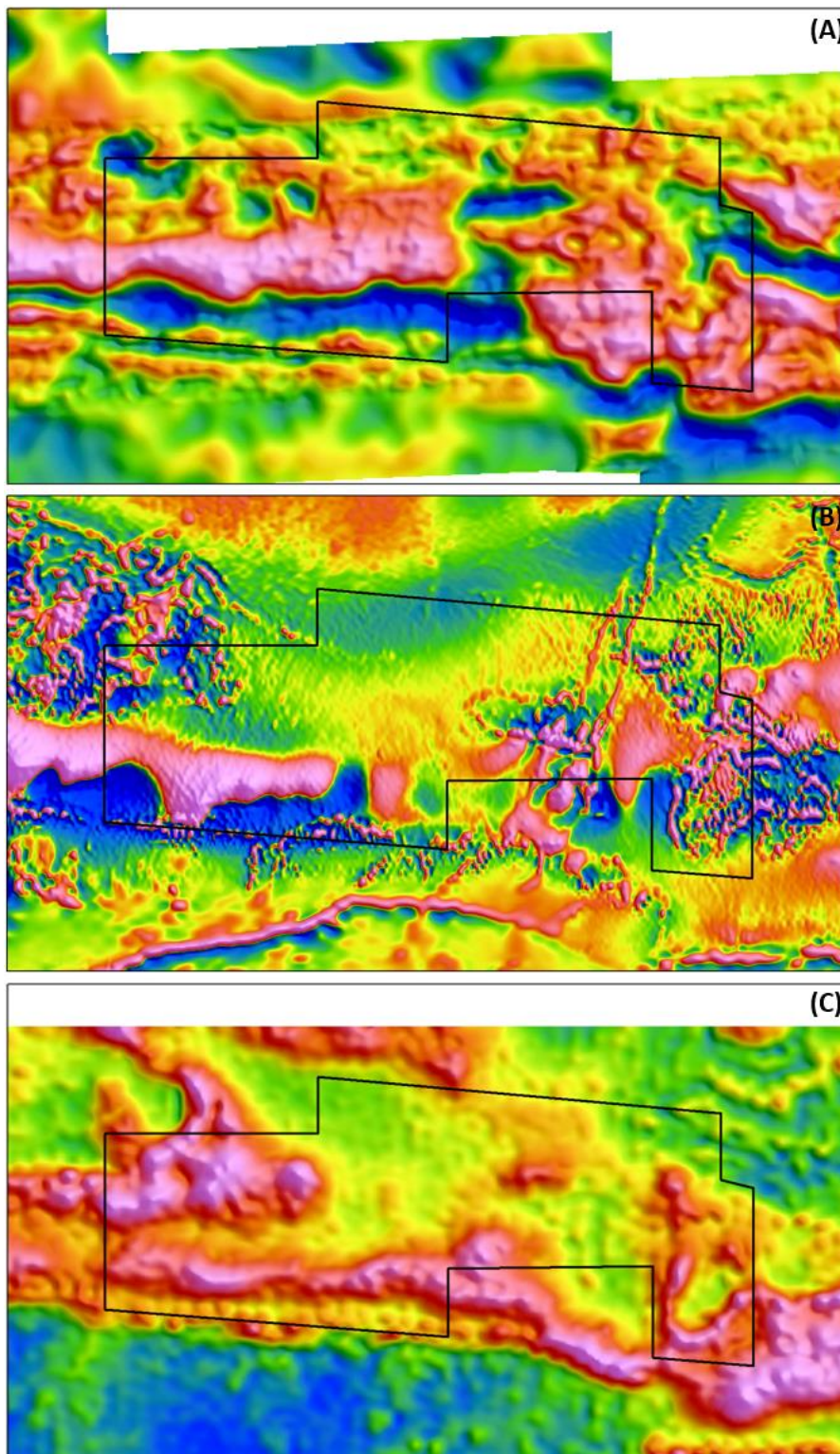

Figure 2. Apriori airborne geophysical datasets. (A) Residual (200m) of the gD of the AGG; (B) 1VD of the RTP of the TMI of the AMAG; (C) Conductivity depth-slice (75m) of the AEM. Passive seismic survey outline shown in black. Hot colours represent high values and cold colours represent low values. Caution must be used when interpreting (B), as low values are negatively oriented/ remanent high values. All images feature histogram equalised colour stretches. Note: legends and coordinates have been deliberately omitted.

PASSIVE SEISMIC DATA

In 2022 and 2023, two passive seismic surveys were acquired using SmartSolo IGU-16HR 3-component 5Hz nodal geophones deployed at a total of ~3,400 locations within the area covered by this paper (Figure 3). Station spacing was 50 m along north-south oriented lines, and 300 m between lines, whilst sample rate was 250 Hz. Geophones were deployed on top of the ground using the optional long spike without any form of wind protection, to minimise ground disturbance and reduce deployment time and cost. Typical recording duration was a brief 15 to 20 minutes to further reduce acquisition time and cost.

Figure 3. Plot of actual passive seismic geophone locations/ stations (black). Survey extents shown in red. Note that coordinates have been deliberately omitted.

The data were processed using the horizontal-to-vertical spectral ratio (HVSR) method. Time series were edited using statistical filters to remove the effects of wind gusts and other spurious noise events of unknown origin. Clean-up steps included the removal of ~30 seconds from start and end of each recording, primarily to eliminate the effects of operator movement. Time series of the horizontal (X and Y) and vertical (Z) ground motion were transformed to spectral velocities using a Fast-Fourier Transform (FFT). H/V spectral ratios were then derived from these spectral velocities and a smoothing function was applied. The HVSR values were normalized over a frequency range of 0.05 to 8 Hz to emphasise resonance energy of greatest interest.

Data quality between geophones was very consistent, with all 28 geophones producing very similar results during tests at the same location at the same time on three different days. The repeatability of data on different days for both tests and survey data were however variable, and often correlated with recorded wind speeds, likely due to the above ground and unshielded deployment. Data between the two surveys shows good continuity along and between lines.

PASSIVE SEISMIC INTERPRETATION

When there are shear-wave velocity (V_s) contrasts, such as such as detrital cover (slow) overlying BIF or WD (fast), vertical and horizontal motion at the ground surface differs. The spectral ratio of the two directions of ground motion produces a resonance peak, the frequency of which is related to the depth of the subsurface boundary (h) using the following equation.

$$h = V_s / 4f_n$$

Vertical seismic profile (VSP) data were planned to be acquired to inform the shear-wave velocities used for depth transformation, however the equipment was not available in time. Although literature-published non-linear regression functions (e.g., Thabet, 2019) could have been used, a constant shear-wave velocity of 500 m/s was used based on the results of previous surveys. Once VSP data are collected in the future, the depths can be corrected using measured in-situ shear-wave velocities, instead of the blanket 500 m/s currently used. This will improve the depth accuracy of the interpreted horizons.

Numerous unpublished surveys and trials using passive seismic with brief recording duration and interpretation of HVSR peaks has shown that results can vary greatly in the Pilbara, particularly when the target is at > 100 m depth. Preliminary results from this survey appeared to be mixed. Two peak horizons ($f_{(p1)}$ and $f_{(p2)}$) were interpreted throughout most of the survey area (Figure 4). The deeper of the two ($f_{(p1)}$) had the best correlation with depth to basement as interpreted from apriori data, however this same horizon had the worst lateral continuity of the two peak horizons. Whilst looking at the sections, the HVSR trough/ minimum ($f_{(t)}$) was identified and observed to be more laterally continuous and have more vertical variability in a controlled manner akin to folding and paleochannels, which piqued the interest of the authors. The trough horizon was then picked, and a literature review conducted to determine to what extent this approach had been previously documented.
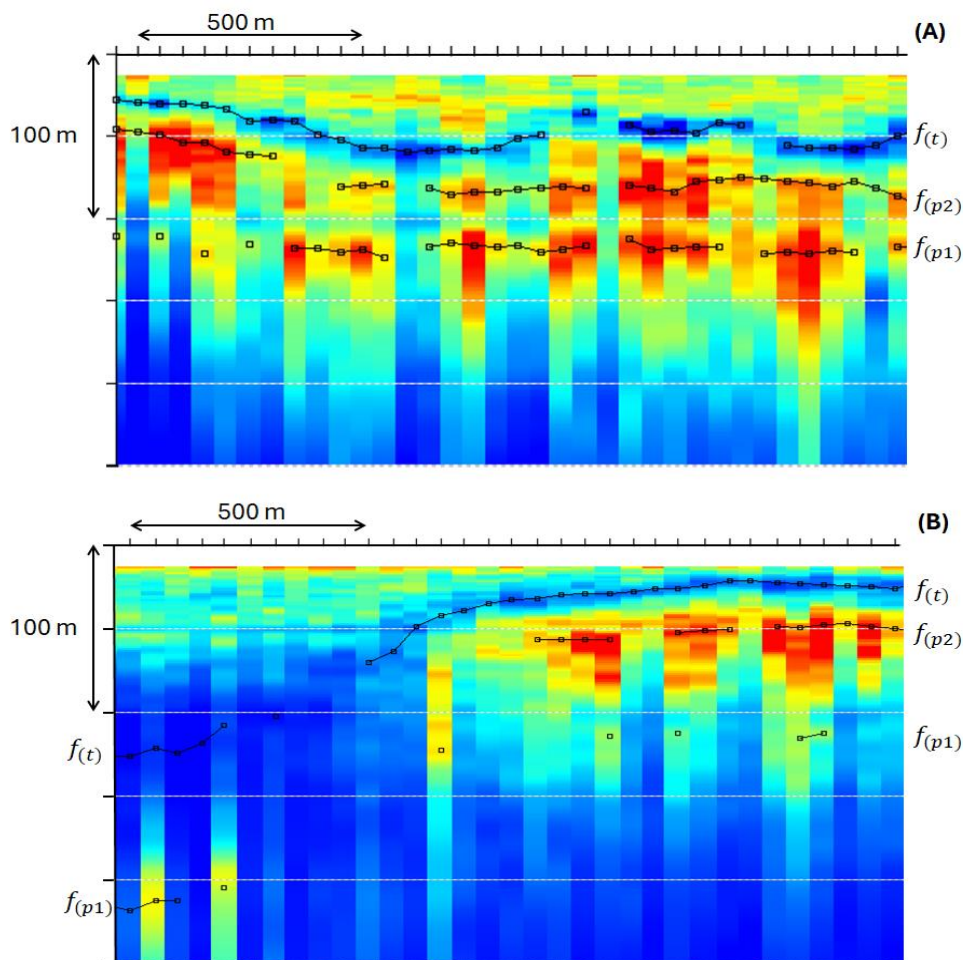

Figure 4. Example of two HVSR sections showing interpreted peak and trough horizons picked. Typically, there was one dominant trough horizon ($f_{(t)}$), and two dominant peak horizons evident ($f_{(p1)}$) and ($f_{(p2)}$). (A) shows a line where all three horizons easily interpreted, whilst (B) shows a line where the peak horizons, particularly the deeper one ($f_{(p1)}$) are largely absent at depth. The trough-horizon shows improved lateral continuity and increased vertical variability relative to the peak-horizons. Note: legends, coordinates and drill data have been deliberately omitted.

Resonance minima, where the HVSR is equal to one, are sometimes seen in HVSR results (e.g., Chandler and Lively, 2014; Riley at al., 2019; Sauck, 2017). These minima typically occur at a frequency double that of a directly adjacent resonance peak (Hinzen et al., 2004) and are likely caused by Raleigh wave interference with the vertically-incident SH waves that generate the peaks (e.g., Konno and Ohmachi, 1998). However, as noted by Sauck (2017), not all resonance peaks have an associated minimum.

Even when a resonance minimum is present, it is often not specifically mentioned or used for interpretation. Indeed, in situations where HVSR peak quality is good, a trough adds limited value. However, as noted by Chandler and Lively (2014), in deep-bedrock situations, the (first) trough frequencies can sometimes produce more reliable depth-to-bedrock values than peaks. One alterative interpretation for a resonance low was presented in Cantwell et al. (2019) who postulated for a HVSR survey in Kazakhstan that a horizon with a distinct resonance low was caused by a velocity inversion.

For the current study, the trough horizon, depth converted using half of the picked frequency, correlates reasonably well with the deeper HVSR peak horizon (Figure 5), The trough horizon displays improved along-line continuity, along-line depth variability and better across-line continuity (Figures 4 and 5). The trough horizon was also able to be interpreted at more passive seismic station (76 %) than the deeper peak horizon ($f_{(p1)}$, 33 %), with the shallower peak horizon ($f_{(p2)}$) picked at 53% of stations (Figure 4). Whilst the shallower peak horizons were picked at more locations, they were not of primary interest, as they appear to correlate with layering within the cover, rather than the cover-basement contact. The deepest peak horizon $f_{(p1)}$ also shows a clear DC shift in depth towards the centre of the survey area, which correlates with stations acquired on different days when there was a notable change in wind conditions. This undesirable effect on the data isn't visible in the trough horizon.
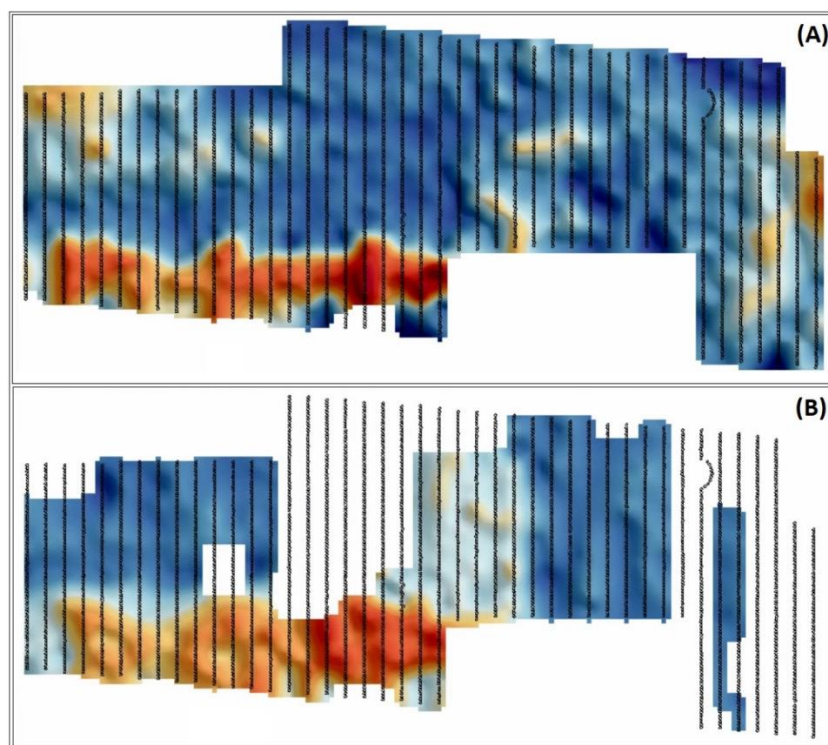

Figure 5. Comparison of the HVSR gridded depth horizons. (A) shows the trough ($f_{(t)}$) and (B) shows the deeper peak ($f_{(p1)}$). Both images share the same linear colour depth stretch. The depths between the two horizons are similar, though the trough horizon (depth generated using half of the picked frequency) shows improved lateral continuity and increased vertical variability relative to the conventional peak-horizons, in addition to being able to be interpreted at more locations. Note: legends and coordinates have been deliberately omitted.

The interpreted HVSR trough horizon varies in depth from approximately 25 to 275 m, being both shallower and deeper than the deepest peak horizon which ranges from 40 to 230 m depth (Figure 5). When viewing the depths as a histogram, there is a large peak in the trough horizon between 50 and 75 m, with a bias towards deeper values, with a reasonable population down to 200 m depth. This compares against the limited drilling reasonably well (given there is currently no velocity control) with depths outside of the paleochannel ranging from 0 to 100 m (typically around 50 m), and the paleochannel typically varying from 100 to 200 m depth and reaching approximately 400 m depth at the eastern end of the large paleochannel. The deepest location of the trough horizon (275 m) is also situated at the eastern end of the large paleochannel.

When comparing the HVSR trough horizon (Figure 5) directly with the individual apriori airborne geophysical datasets (Figure 2), there is a strong spatial correlation with the residual of the gD of the AGG, where low residual density values correlate with deeper HVSR trough horizon, suggesting that the cover has a lower density than the underlying metasediment stratigraphy (as expected). When compared to the conductivity data from the AEM and the AMAG data, various additional correlations can be seen, though not to the extent of the AGG data.

The depth to the interpreted HVSR trough horizon (Figure 5) shows excellent correlation with the integrated under-cover geological interpretation generated from the apriori AGG, AEM, and AMAG data (Figure 1), as seen in Figure 6. The large east-west paleochannel in the southwest correlates well with the deepest anomaly in the HVSR trough horizon, as is the case in the east along the large fault shear-zone. To the northwest and southeast, the BKM BIF consistently shows as a moderate to deep trough horizon. The HVSR method is likely responding to the McRae Shale found at the base of this formation, hence the deeper depths and larger footprint in the northwest where the BKM BIF

is present as a syncline. The WD consistently shows up as a shallow to moderate depth anomaly in the HVSR trough horizon. The intrusive domes in the centre, the mildly outcropping MM BIF in the south, and the outcropping BIF not mapped in the far northeast corner beyond the large fault zone all show for the most part as very shallow depths in the HVSR trough horizon, though not as consistently as with the other geology. Note the passive seismic data interpretation shown in Figures 4 and 5 was done blind to the apriori integrated geophysical interpretation shown in Figure 1. Neither dataset shown in Figure 6 is influenced by the other.
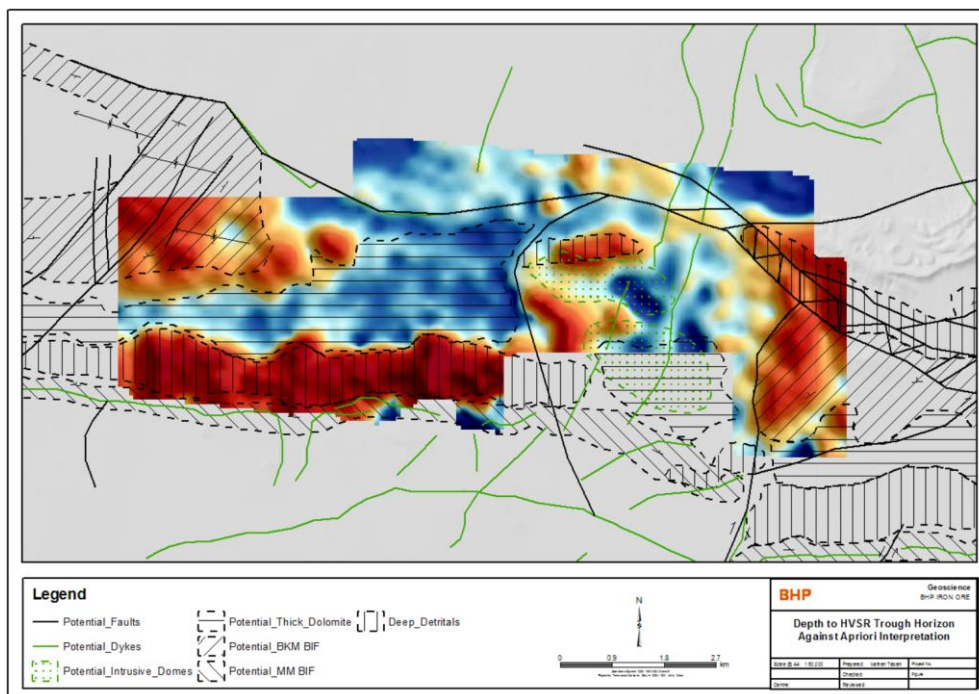

Figure 6. Comparison of depth to the HVSR trough horizon shown against apriori integrated undercover geological interpretations of airborne geophysical data (Figure 1). Hot colours represent deeper depths whilst cold colours represent shallower depths (histogram equalised stretch). Note the strong correlation between apriori interpretation and the depth to the HVSR trough horizon (which was picked without knowledge of the apriori geological interpretation). Note coordinates and the HVSR trough horizon colour legend have been deliberately omitted.

CONCLUSIONS

Short duration 3-component passive seismic survey datasets are typically interpreted by picking HVSR frequency peaks/ maximums and then converted to depths with an assumed shear-wave velocity, when low-cost and rapid results are desired. Whilst this method generally produces acceptable results throughout Australia, the results have been mixed in the Pilbara with its challenging geology. In this study, we picked HVSR troughs/ minimums in the data and converted these to depth using half their frequency. The HVSR trough horizon discussed in this paper was easier to interpret, had better along-line and across-line continuity, and more vertical variability than the corresponding peak horizon.

The HVSR trough horizon shows excellent correlation with independent undercover geological interpretations generated from various apriori, mostly airborne geophysics datasets spatially in plan-view, and aligns well with limited drilling with respect to depth. Deep paleochannels and stratigraphy were characterised well in plan-view and section-view, whilst structures and intrusions were sometimes visible, but less so.

Once vertical seismic profile (VSP) data is available, the depth transformations will be re-calculated using the more accurate and granular shear-wave velocity, instead of the assumed constant shear-wave velocity used, which will improve the accuracy of the derived basement surface.

All existing and future 3-component passive seismic HVSR datasets could be interpreted for HVSR troughs, converted to depth using half the trough frequency, and assessed for its potential to deliver improved results relative to the conventional peak horizon(s) for little additional cost/ time. This should be prioritised for surveys were signal to noise was poor and/ or the basement contact is > 100 m depth, as this appears to be where the trough method becomes particularly advantageous.

REFERENCES

BHP, 2023, Water: https://www.bhp.com/sustainability/environment/water.

Cantwell, N., Owers, M., Meyers, J., and Riley, S., 2019. Case studies on the application of passive seismic horizontal to vertical spectral ratio (HVSR) surveying for heavy mineral sand exploration. ASEG Extended Abstracts, 2019(1). https://doi.org/10.1080/22020586.2019.12073142.

Chandler, V.W, and Lively, R.S., 2014. Evaluation of the horizontal-to-vertical spectral ratio (HVSR) passive seismic method for estimating the thickness of quaternary deposits in Minnesota and adjacent parts of Wisconsin: Minnesota geological Survey, Open file report 14-01.

Duuring P., Hagemann, S.G., Laukamp, C., and Chiarelli, L., 2019. Supergene modification of magnetite and hematite shear zones in banded iron-formation at Mt Richardson, Yilgarn Craton, Western Australia, Ore Geology Reviews, Volume 111. https://doi.org/10.1016/j.oregeorev.2019.102995

Hinzen, K.G., Weber, B., and Scherbaum, F., 2004. On the resolution of H/V measurements to determine sediment thickness, a case study across a normal fault in the Lower Rhine Embayment, Germany. Journal of Earthquake Engineering, Volume 8, pp. 909-926. https://doi.org/10.1080/13632460409350514

Kepert, D.A., 2018. The mapped stratigraphy and structure of the Mining Area C region, Hamersley Province: Geological Survey of Western Australia, Report 185.

Konno, K., and Ohmachi, T., 1998. Ground-motion characteristics estimated from spectral ratio between horizontal and vertical components of microtremor. Bulletin of the Seismological Society of America, Volume 88, pp. 228-241. https://doi.org/10.1785/BSSA0880010228.

Lane, J.W., Jr., White, E.A., Steele, G.V., and Cannia, J.C., 2008. Estimation of bedrock depth using the horizontal-to-vertical (H/V) ambient-noise seismic method. Symposium on the Application of Geophysics to Engineering and Environmental Problems, 13 p. https://doi.org/10.4133/1.2963289.

Riley, S., Meyers, J., and Sinnott, J., 2019. Passive seismic HVSR surveying for groundwater exploration at the Chilalo Graphite Project, Tanzania. ASEG Extended Abstracts, 2019(1). https://doi.org/10.1080/22020586.2019.12073155

Sauck, W.A., 2017. The HVSR passive seismic method evaluated in several regions of Brazil. SEG Global Meeting Abstracts: 641-645. https://doi.org/10.1190/sbgf2017-126

Thabet, M., 2019. Site-specific relationships between bedrock depth and HVSR fundamental resonance frequency using KiKNET data from Japan. Pure and Applied Geophysics, Volume 176, p. 4809-4831. https://doi.org/10.1007/s00024-019-02256-7